STM JOURNALS

Emerging Trends in
Chemical Engineering

ISSN: 2349-4786
Volume 12, Issue 3, 2025
September–December
DOI (Journal): 10.37591/ETCE

https://journals.stmjournals.com/etce

Research ETCE

Design of Plant for the Production of 30,000 Tons Per Year Capacity of Dimethyl Carbonate (DMC) from Natural Gas Using Aspen HYSYS

Beker Benjamin[1], ThankGod Oweifea GoodHead[2], Chukwuemeka Peter Ukpaka[3,*]

Abstract

This study focuses on the design of a plant for the production of 30,000 tons per year of dimethyl carbonate (DMC) from natural gas. The plant design was carried out using the Aspen HYSYS Software. The data obtained from Kokori natural gas served as the primary feedstock for the plant. A kinetic model for the production of DMC was developed from existing literature, followed by the development of the mathematical model of a packed bed reactor. The simulation of the DMC plant model was done using Aspen HYSYS software. DMC is a widely utilized liquid chemical with diverse applications ranging from transportation fuel and energy. The planned DMC production plant was designed to employ the methanol dehydration method for synthesizing 30,000 metric tons of DMC annually. The primary feedstock used in the process is natural gas. Methanol is synthesized from natural gas, and then DMC is produced from the dehydration of methanol in the second step. The methodology involves the compression of natural gas to extract methane, followed by dry reforming to produce syngas, methanol synthesis, and subsequent conversion to DMC. For the simulation of DMC production from natural gas in this study, a flow rate of 3847 kg/h of natural gas (feed) was supplied with a temperature and pressure of 30°C and 10 bar, respectively, at the plug flow reactor (PFR). The DMC was produced at the conversion reactor where methanol and carbon dioxide (CO_2) were synthesized at a temperature and pressure of 162.7°C and 60 bar, respectively. The DMC production was optimized at a methanol conversion rate of 80% to yield DMC. Material and Energy balance, development of models, and sizing of major equipment of the plant were considered. For the cost estimation and economic evaluation for the first year, an estimated capital investment of approximately 2,823,220 USD and an operating cost of 1,506,050 USD/year will be required. The establishment of the plant is anticipated to yield encompassing job creation, increased tax revenue, and local economic development. Overall, the proposed project plant holds significant potential and annually produces 30,000 t of 95% pure DMC from natural gas.

***Author for Correspondence**
Chukwuemeka Peter Ukpaka
E-mail: chukwuemeka24@yahoo.com

[1]Research Student, Department of Chemical/Petrochemical Engineering, Rivers State University, P.M.B. 5080, Nkpolu-Oroworokwo, Port Harcourt, Nigeria
[2]Associate Professor, Department of Chemical/Petrochemical Engineering, Rivers State University, P.M.B. 5080, Nkpolu-Oroworokwo, Port Harcourt, Nigeria
[3]Professor, Department of Chemical/Petrochemical Engineering, Rivers State University, P.M.B. 5080, Nkpolu-Oroworokwo, Port Harcourt, Nigeria

Received Date: September 24, 2025
Accepted Date: October 03, 2025
Published Date: October 24, 2025

Citation: Beker Benjamin, ThankGod Oweifea GoodHead, Chukwuemeka Peter Ukpaka. Design of Plant for the Production of 30,000 Tons Per Year Capacity of Dimethyl Carbonate (DMC) from Natural Gas Using Aspen HYSYS. Emerging Trends in Chemical Engineering. 2025; 12(3): 45–60p.

Keywords: Dimethyl carbonate, natural gas, plant, design, methanol, simulation

INTRODUCTION

Dimethyl carbonate (DMC) has recently been discovered as an alternative sustainable transportation fuel. It is an important green and industrial chemical because it is environmentally friendly and possesses the ability for multiple reactivity and applications. Power-to-Fuel is an emerging concept that uses surplus electricity-powered H_2 and CO_2 to produce future fuels. Previously studied fuel candidates included methanol, Fischer-Tropsch, and ethers. Apart from

© STM Journals 2025. All Rights Reserved

these candidates, dimethyl carbonate (DMC) is increasingly recognized as a viable fuel. One of the main causes of climate change is the increase in the concentration of greenhouse gases, and among the greenhouse gases currently emitted, CO_2 accounts for the largest share at 77% [1].

Dimethyl carbonate (DMC) can be used for different purposes, such as a solvent, methylating agent, fuel additive, but it also finds an application in polycarbonate production. The direct synthesis of DMC from CO_2 and methanol seems to be an interesting alternative compared to the utilization of toxic phosgene, which could lead to the sustainable production of polycarbonate as the ultimate product. From a study published in 2020, a high-level conversion (85.2%) can be reached with a zirconium (IV) acetylacetonate catalyst, leading to carboxymethylation with a selectivity up to 99% [2].

The design and simulation of the synthesis of dimethyl carbonate and the product separation process plant were carried out. In the study, a reactive distillation column was considered in the production of dimethyl carbonate. The catalytic distillation (CD), which is also known as reactive distillation (RD), that combines the heterogeneous catalysed chemical reaction and the distillation in a single unit, has attracted more interest in academia and become more important in the chemical processing industry as it has been successfully used in several important industrial processes. The CD provides some advantages such as high conversion more than the chemical equilibrium, energy saving, overcoming the azeotropic limitations, and prolonging the catalyst lifetime. The number of contributions both for the simulative and experimental investigations about catalytic distillation has greatly increased in recent years, especially for the modelling and simulation studies [3]. The system of the DMC synthesis process in a CD column mainly involves four components: methanol, DMC, MC, and ammonia, as the first step reaction was omitted in the distillation column. The boiling points of the pure components at atmospheric pressure were ranged as follows: methanol 337.66 K; DMC 363.45 K; MC 450.2 K; and ammonia (NH_3) 239.72 K. It could be seen that MC should almost exist in the liquid phase in the CD process under high pressure, and the reactions would take place in the liquid phase in a CD reaction zone. Since the system included a non-condensable component of ammonia and a binary azeotropic pair of methanol-DMC, it shows strong non-ideal properties, and the vapor-liquid equilibrium was calculated by the EOS + activity method [4].

In this work, the systematic hierarchical decomposition design method consisting of 12 tasks as described is employed to design a process producing 100,000 Mt of 99% pure DMC per year with an additional production of 73,000 Mt of ethylene glycol (EG) of 91% purity. This method assists in constructing the process, initially obtaining a base case and subsequently developing an optimized rigorous design. Data required to develop a plant of the desired capacity is assimilated in tasks 1–3 to facilitate preliminary design decisions. Those are then verified through a mass balance in task 4 employing the commercial design simulator PROII. The simulation is extended from the initially simple model to a rigorous one in tasks 5–6, leading to a full-fledged rigorous model where mass and energy balances are confirmed in task 7. The process is then sized, and an economic analysis is carried out with the software ECON in tasks 8–9, leading to a base case for the process. Through that, targets for improvement are identified, and the process is improved through optimization and heat integration in tasks 10–12. This is followed by an environmental impact analysis after each improvement step, to assess the overall sustainability of the final design [5]. Applying these last tasks enables the design of an economically viable and simultaneously sustainable process for obtaining DMC. From an environmental standpoint, apart from the utilization of CO_2, equivalent to a net reduction of CO_2 emissions, the focus is set to reducing waste. This is achieved by handling the azeotropes by minimizing the use of solvents, which makes the separations environmentally benign. The process is made economically more attractive by mass integration through recycling EC and heat integration to use energy efficiently. Through this hierarchical decomposition method, a potential zero-discharge closed-loop system is designed through the recycling of CO_2 produced from the hydrothermal decomposition of EG-EC azeotrope [6].

© STM Journals 2025. All Rights Reserved

MATERIALS AND METHODS

The materials that will be used for this research work include:

1. Aspen HYSYS Software;
2. Chemical Engineering Handbook; and
3. Natural gas compositions from three different oil field names: Kokori Field, Utorogu Gas Plant, and Sapele West Field in Delta State.

Methods

1. Mathematical modeling methods; and
2. Process simulation method.

Kinetic Model Development

The kinetics for the direct synthesis of DMC from CO_2 and methanol using a highly active catalyst have been developed and will be obtained from the literature. Developed a reaction kinetic model to produce synthesis gas from dry methane reforming. The reaction can be written as follows:

$$\mathrm{CH_4 + CO_2 \rightarrow 2CO + 2H_2} \quad (1)$$

The reaction rate can be expressed as:

$$r_i = KC_AC_B \quad (2)$$

Where:

$$K = Ae^{-\frac{E}{RT}} \quad (3)$$

C_A= concentration of methane, C_B= concentration of carbon dioxide, r_i= rate of reaction, K= rate constant, A= pre exponential constant or frequency factor, E= activation energy T = temperature.

This reaction is carried out at a temperature range of 650 to 850°C. The values of A and E are to be determined experimentally.

The kinetics for the hydrogenation of CO to produce methanol, which is the second reaction according to which:

$$CO + 2H_2 \rightarrow CH_3OH \quad (4)$$

The mechanisms for the rate-determining step and the corresponding rate of reaction are given in Table 1.

Lastly, the final reaction for the synthesis of methanol and CO_2 to produce DMC, as stated in the work, is given by the reaction:

$$\mathrm{2CH_3OH + CO_2 \rightarrow CH_3OCOOCH_3 + H_2O} \quad (5)$$

The rate expression is given by:

$$r = K[CO_2]^a[CH_3OH]^b \quad (6)$$

K is the rate constant, and a, and b, are experimentally determined constants. While the rate constant is strictly controlled by the temperature, pressure, activation energy, and activation volume, the overall rate is also a function of the concentration of reactants and catalyst loading [7]. To estimate the order of the reaction with respect to each reagent, we conducted a series of initial rate experiments in which the loading of ceria and the amount of methanol were varied while maintaining a constant 2000 psi reaction pressure, consistent amounts of CO_2, and a consistent reaction temperature of 125°C. Since the initial rate region remains well behaved and linear for well over 60 min at these conditions, the reaction was stopped at 30 or 60 min for each initial rate experiment to produce DMC [8].

Development of Model Equations for Packed Bed Reactor

This section will develop the mathematical model of the packed bed reactor using the law of conservation of mass and energy from first principles [9].

© STM Journals 2025. All Rights Reserved

Table 1. Rate-determining step and corresponding rate equation.

Model no.	Rate controlling process	Proposed rate equation
	Carbide mechanism	
1	the $CS + HS \overset{k_{Cl}}{\rightarrow} HCS + S$	$-r_{CO} = \frac{k_1 P_{CO}^{1/2} P_{H_2}^{1/2}}{\left(1 + K_1 P_{H_2}^{1/2} + K_2 P_{CO}^{1/2}\right)^2}$
2	$H_2 + 2\,S \overset{k_H}{\rightarrow} 2HS$	$-r_{co} = \frac{k_1 P_{H_2}}{\left(1 + K_2 P_{\%0}^{1/2}\right)^2}$
3	$CO + 2\,S \overset{kco}{\rightarrow} CS + OS$	$-r_{Co} = \frac{k_1 P_{CO}}{\left(1 + K_1 P_{H_2}^{1/2} + K_2 P_{CO} P_H^{-1/2}\right)^2}$
4	$HCS + HS \overset{k_{C2}}{\rightarrow} H_2CS + S$	$-r_{CO} = \frac{k_1 P_{CO}^{1/2} P_{H_2}^{3/4}}{\left(1 + K_{H_2}^{1/2} + K_2 P_{Co}^{1/2} P_{H_2}^{-1/4} + K_3 P_{Co}^{1/2} P_{H_2}^{1/4}\right)^2}$
5	$CS + HS \overset{k_{C1}}{\rightarrow} HCS + S$ $HOS + HS \overset{ko_2}{\rightarrow} H_2OS$	$-r_{CO} = \frac{k_1 P_{CO}^{1/2} P_{H_2}^{3/2}}{\left(1 + K_1 P_{H_2}^{1/2} + K_2 P_{CO}^{1/2} P_{H_2}^{-1/4} + K_3 P_{CO}^{1/2} P_{H_2}^{1/2}\right)^2}$
6	$HCS + HS \overset{k_{C2}}{\rightarrow} H_2CS + 2\,S$ the $HOS + HS \overset{koz}{\rightarrow} H_2O + S$	$-r_{CO} = \frac{k_1 P_{CO}^{1/2} P_{H_2}}{\left(1 + K_1 P_{H_2}^{1/2} + K_2 P_{CO}^{1/2} + K_3 P_{CO}^{1/2} P_{H_2}^{1/2}\right)^2}$
	Enolic mechanism	
7	$OCS + HS \overset{k_{OH1}}{\rightarrow} HOS + S$	$-r_{CO} = \frac{k_1 P_H^{\frac{1}{2}} P_{CO}}{\left(1 + K_{CO} P_{CO} + K_1 P_{H_2}^{\frac{1}{2}}\right)^2}$
8.	$HOCS + HS \overset{k_{OH2}}{\rightarrow} H_2O + CS + S$ $OCS + HS \overset{k_{oh1}}{\rightarrow} HOS + S$	$-r_{CO} = \frac{k_1 P_{CO} P_{H_2}}{\left(1 + K_1 P_{H_2}^{1/2} + K_{CO} P_{CO} + K_2 P_{CO} P_{H_2^2}^{1/2}\right)^2}$ $-r_{CO} = \frac{k_1 P_{H_2}^{1/2} P_{CO}}{\left(1 + K_{CO} P_{CO} + K_1 P_{H_2}^{1/2}\right)^2}$

Modelling Assumptions

1. The process is assumed to operate at steady state conditions.
2. The flow condition in the reactor is assumed as plug flow.
3. Concentration of reactants varies along the length of the reactor from point to point.
4. Dispersion effects are neglected in the direction of flow.
5. The process is assumed to be isothermal.
6. The pressure drops in reactors and columns are negligible.

Material Balance

Consider a cylindrical volume element within a packed bed reactor, as depicted in Figure 1.

The material balance model will include the following assumptions:

1. Steady state operations.
2. Negligible axial and radial dispersion.
3. Negligible interface mass resistance.
4. Negligible radial velocity gradient.

© STM Journals 2025. All Rights Reserved

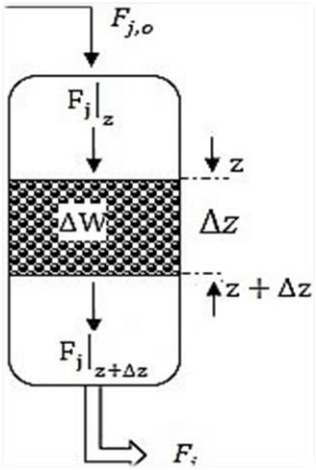

Figure 1. Material balance schematic of a packed bed reactor.

By considering the elemental volume and applying the principle of conservation of mass, we can express the general material balance equation as follows:

$$\left[\begin{array}{c}\text{Rate of inflow}\\ \text{of specie to}\\ \text{volume element}\\ \text{per time } \left(\frac{\text{Mol}}{\text{s}}\right)\end{array}\right] - \left[\begin{array}{c}\text{Rate of outflow}\\ \text{of specie from}\\ \text{volume element}\\ \text{per time } \left(\frac{\text{Mol}}{\text{s}}\right)\end{array}\right] + \left[\begin{array}{c}\text{Rate of generation}\\ \text{of specie within}\\ \text{volume element}\\ \text{per time } \left(\frac{\text{Mol}}{\text{s}}\right)\end{array}\right] = \left[\begin{array}{c}\text{Rate of accumulation}\\ \text{of specie within}\\ \text{volume element}\\ \text{per time } \left(\frac{\text{Mol}}{\text{s}}\right)\end{array}\right] \quad (7)$$

Dividing by Δz and taking the limit as Δz→0:

$$\frac{dF_j}{dz} = \rho_B . A_c \sum_{i,j}\left(v_{i,j}\eta_i r_i\right) \quad (8)$$

Where:

F_j: Molar flow rate of component j in kmol/hr, z: Reactor height in m, ρ_B: Bed density of the reactor in $Kgcat/m^{-3}$, A_c: Cross-sectional Area in m^2, $v_{i,j}$: Stoichiometric coefficient of component j in reaction, η: Effectiveness factor of the catalyst, r_i: Rate of reaction in $kmol.\,kgcat^{-1}\,hr^{-1}$ [10].

Energy Balance

Examine a differential volume illustrated in Figure 2. The energy balance relies on the principle of conservation of energy or the first law of thermodynamics.

The energy balance model will incorporate the following assumptions:

1. Negligible changes in kinetic energy.
2. Negligible changes in potential energy.
3. Negligible shaft work.
4. Operation in a steady state.

$$\left[\begin{array}{c}\text{Energy}\\ \text{input into volume}\\ \text{element}\end{array}\right] - \left[\begin{array}{c}\text{Energy}\\ \text{output from volume}\\ \text{element}\end{array}\right] \pm \left[\begin{array}{c}\text{Energy}\\ \text{generation}\\ \text{or consumption}\\ \text{within volume}\\ \text{element}\end{array}\right] \pm$$

© STM Journals 2025. All Rights Reserved

$$\begin{bmatrix}\text{Energy added}\\ \text{or loss to surrounding}\\ \text{to or from volume element}\end{bmatrix} = \begin{bmatrix}\text{Energy}\\ \text{accumulation}\\ \text{within volume element}\end{bmatrix} \quad (9)$$

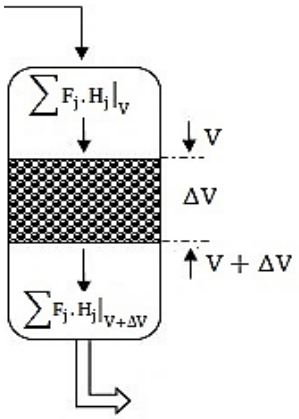

Figure 2. Energy balance schematic of a packed bed reactor.

Expressing each term as follows:
Dividing byΔV, taking limiting as $\Delta V \rightarrow 0$ and simplifying:

$$\sum_j F_j . C_{P_j} \frac{dT}{dV} = \rho_B . \sum_{i,j} \{(\Delta H_{R_i}) . v_{i,j} . \eta_i . r_i\} - \sum_j C_{P_j} \frac{dF_j}{dV} (T + \Delta T - T_{ref}) - \frac{U_a . \pi d_t \Delta z . (T_w - T)}{\Delta V} \quad (10)$$

Where:
C_{P_j}: Specific heat capacity component j in $JK^{-1}\,mol^{-1}$, ΔH_{Ri}: Change in enthalpy of reaction i in $Jmol^{-1}$, T: Temperature in K, T_w: Temperature of the reactor wall in K, U_A: Heat transfer coefficient, d_t: Diameter of the reactor in m

Solution Technique

Aspen HYSYS Model Process Flow Diagram

Figure 3 shows the process flow diagram (PFD) of the DMC plant model built and simulated using Aspen HYSYS software version 14. The first part of the simulation started with compressing the natural gas from the field, which was then heated inside a heater then passed into a component separator to split out methane from the other gases [11, 12]. The methane stream was then mixed with the CO_2 gas stream before being sent to the first reactor, where the reaction of methane and CO_2 to produce CO and H_2 takes place. The products from reactor 1 were cooled and sent to the second reactor, where the reaction of CO and H_2 to produce methanol occurs. The products coming out of the second reactor were sent to a component splitter to separate pure methanol from the reactor product, which was then mixed with a stream of CO_2 gas and sent to the third reactor, where the reaction of methanol and CO_2 to produce DMC product occurs. The DMC product from the third reactor was sent to a component separator to separate DMC, which was then stored in a storage tank [13].

Input Data

The data for the simulation are presented in Table 2.

Table 2 shows the natural gas compositions from three different oil fields, namely: Kokori field, Utorogu gas plant, and Sapele West field.

RESULTS AND DISCUSSION

Material balance for DMC plant which consist of three main reactions before the production of DMC product, the first reaction occurs between methane from natural gas with CO_2 to produce CO and

© STM Journals 2025. All Rights Reserved

Hydrogen which is also known as dry reforming of methane, while the second reaction occurs between CO and Hydrogen to produce methanol and is often called methanol synthesis reaction and the last reaction occurs between methanol and CO_2 to produce the desired product DMC also known DMC synthesis reaction, as shown in Table 3 [14].

Energy Balance Result

Energy balance for DMC plants, which consist of process parameters such as temperature, pressure, molar enthalpy, molar entropy, and the heat flow for each unit of the DMC plant [15]. The purpose of carrying out energy balance is to ensure that heat energy is balanced across each unit of the plant in line with the principles of conservation of energy for a steady state process, which simply states that the inflow of energy must be equal to the outflow of energy for that process, as shown in Table 4 [16].

Energy Balance Result

Energy balance for the DMC plant, which consists of process parameters such as temperature, pressure, molar enthalpy, molar entropy, and the heat flow for each unit of the DMC plant. The purpose of carrying out energy balance is to ensure that heat energy is balanced across each unit of the plant in line with the principles of conservation of energy for a steady state process, which simply states that the inflow of energy must be equal to the outflow of energy for that process [17].

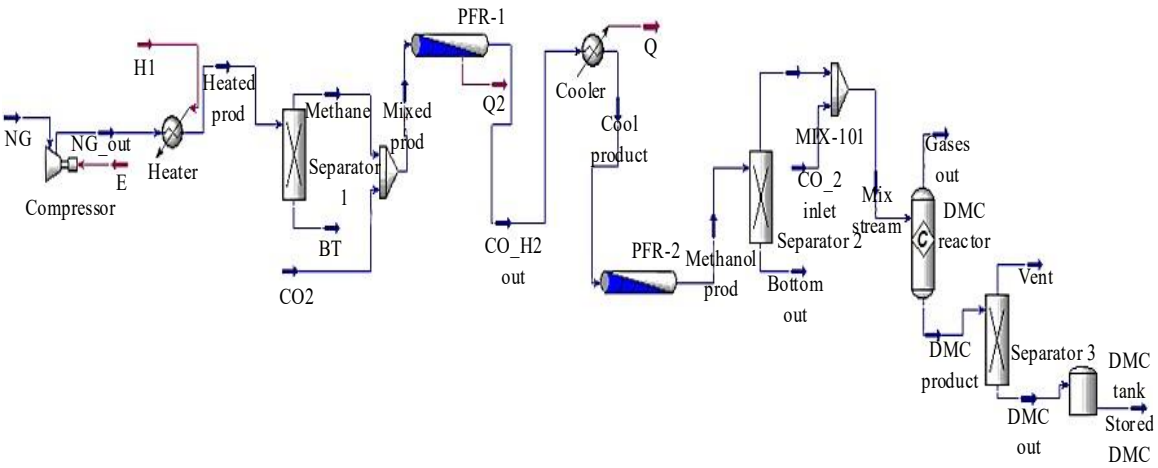

Figure 3. Aspen HYSYS process flow diagram of the DMC plant.

Table 2. Natural gas data from three oil fields.

Component	Kokori field (mol%)	Utorogu gas plant (mol%)	Sapele West Field (mol%)
Methane	68.42	90.19	68.14
Ethane	7.65	6.94	14.22
Propane	11.27	2.09	10.27
n-Butane	4.00	0.361	3.23
i-Butane	4.42	0.414	2.38
n-Pentane	0.94	0.005	0.75
i-pentane	1.55	0.007	1.07
Hexane	0.18	-	-
Nitrogen	0.16	-	-
Carbon-dioxide	1.02	-	-

© STM Journals 2025. All Rights Reserved

Process Optimization

Figure 4 shows the effect of increasing the conversion of methanol on the yield of DMC product. From Figure 4, as the conversion of methanol increased from 10 to 80%, this caused a corresponding increase in the yield of DMC from 0.0256 to 0.4115, but as soon as the conversion of methanol was increased beyond 80%, that is, 90 and 95% respectively, the yield of DMC dropped to 0.3870 and 0.3115, respectively. The reason for this behavior is that when a reaction is reversible, increasing the conversion beyond a certain point might push the reaction towards equilibrium, where the reverse rate increases, leading to a decline in the desired product's mole fraction. From Figure 4, the optimum conversion needed to achieve a yield of 0.4115 DMC is 80%. This trend is in line with the earlier work [18].

Table 3. Material balance summary sheet.

Equipment	Input stream (kg/h)	Output streams	Top stream (kg/h)	Bottom stream (kg/h)
Compressor	3847		3847	
Heater	3847		3847	
Separator 1	3847		1656	2191
Mixer 1	1656		4401	6057
PFR1	6057		6057	
Cooler	6057		6057	
PFR2	6057		6057	
Separator 2	6057		3204	2853
Mixer 2	3204		4401	7605
DMC Reactor	7605		4537	3068
Separator 3	4537		1298	3239
DMC Tank	3239		3239	

Table 4. Equipment energy result.

Equipment	Duty (kJ/h)	Source
Compressor	1.335×10^{7}	Electricity
Heater	9.160×10^{6}	Electricity
Cooler	6.898×10^{6}	Electricity

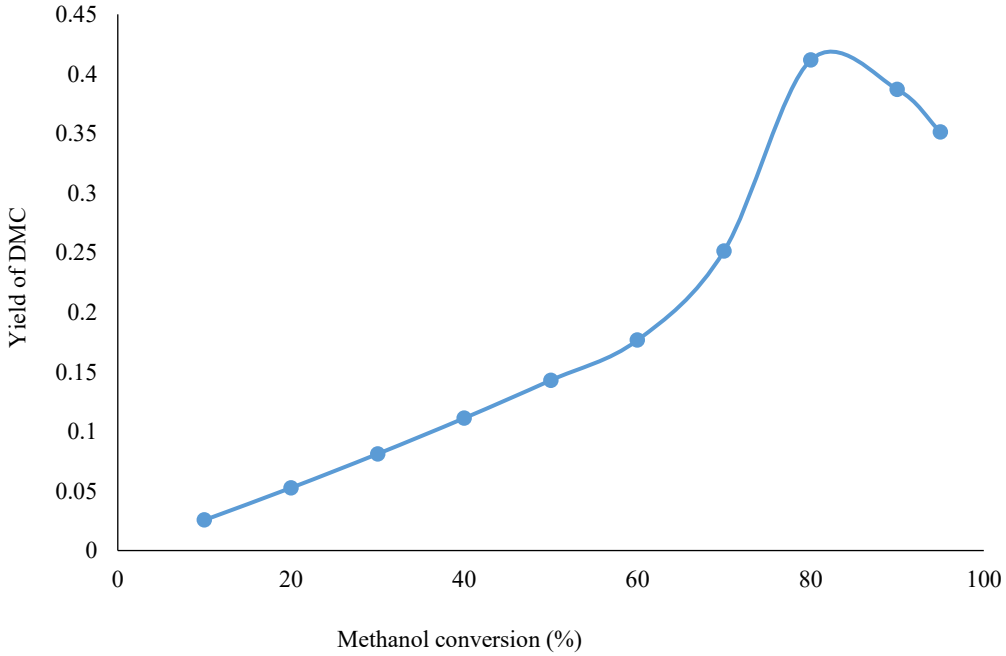

Figure 4. Yield of DMC versus fractional conversion.

© STM Journals 2025. All Rights Reserved

Validation of Model Results

The validation of the model results obtained in this work is shown in Table 5.

The results obtained in this study, as shown in Table 5, were validated against literature data reported. A comparison of the two sets of results shows good agreement, with only moderate deviations that can be attributed to differences in operating conditions, feed ratios, and model assumptions. The reactor temperature predicted in this work was 434.7 K, which is slightly higher than the 393.2 K. This difference of approximately 41 K can be explained by variations in heat management strategies. In the present study, the exothermicity of the reaction was allowed to raise the system temperature more significantly, whereas Hou *et al*. likely employed stricter thermal control or heat removal, resulting in a lower reported operating temperature. Despite this difference, both values lie within the typical temperature window for dimethyl carbonate (DMC) synthesis, thereby confirming the reliability of the model predictions. The reactor pressure in this work was 5000 kPa, compared to 4978 kPa in the literature. The difference is negligible, amounting to less than 0.5%, which validates the thermodynamic assumptions and process conditions adopted in this study. This close agreement shows that the pressure conditions applied are consistent with those typically reported for DMC synthesis, lending credibility to the simulation framework. In terms of conversion, this work predicted a methanol conversion of 95%, which is slightly higher than the 90%. The improved conversion may be attributed to the reactor configuration, catalyst activity, or feed conditions applied in this study. Nonetheless, both values indicate high conversion efficiency, and the 5% difference is within the expected range of variability between different experimental or modeling approaches. This comparison demonstrates that the present model provides a realistic estimation of methanol utilization in DMC synthesis. The yield of DMC in this work was 0.42, compared to 0.39. The higher yield obtained here can be correlated with the higher methanol conversion achieved, as well as the optimized stoichiometric conditions employed. Although there is a slight increase in yield, the results are consistent, with both values showing that DMC production remains below 50% due to side reactions and equilibrium limitations inherent in the process [19].

Profile Plot of Reactor

The temperature profile in Figure 5 depends strongly on whether the reaction is exothermic or endothermic. In exothermic reactions, the temperature rises rapidly near the inlet where the reaction rate is highest. For example, with a heat of reaction of –100 kJ/mol and a feed temperature of 300 K, the reaction of 1 mol/l of reactant in the first 2 sec could release enough energy to increase the outlet temperature to approximately 350 K in an adiabatic system. This rise in temperature accelerates the reaction rate through the Arrhenius relationship but may also lead to hot spots that compromise safety and catalyst stability. Conversely, for an endothermic reaction with a heat demand of +80 kJ/mol, the outlet temperature could drop from 300 K to about 270 K if no external heating is provided. Thus, the temperature profile governs not only the kinetics but also the thermal management strategies required for safe and efficient operation [20].

Table 5. Validating this work with literature.

Parameter	This Work	Hou *et al*., 2022 [12]
DMC reactor temperature (K)	434.7	393.2
DMC reactor pressure (kPa)	5000	4978
Conversion of methanol (%)	95	90
Yield of DMC (–) are unitless ratios	0.42	0.39
Reactant ratio	1:1	1:2

© STM Journals 2025. All Rights Reserved

In Figure 6, the molar entropy of the reacting system typically changes along the reactor length as a function of both reaction progress and temperature evolution. Entropy, being a measure of disorder or energy dispersal, is affected by variations in concentration, composition, and thermal conditions within the reactor. Unlike concentration and conversion profiles that directly track the consumption of reactants, the molar entropy profile provides insight into the thermodynamic driving forces and the irreversibility of processes occurring within the reactor. For an exothermic reaction, the release of heat to the system may increase the local temperature significantly, which in turn raises entropy because entropy is directly proportional to temperature through the relation. For instance, if the temperature rises from 300 K at the inlet to 350 K at the mid-length of the reactor, the molar entropy of the reacting mixture can increase by several joules per mole per kelvin, depending on the heat capacity of the mixture. At the same time, as reactants are consumed and products are formed, the configurational entropy changes due to the redistribution of molecular species. In gas-phase systems, if the number of moles of products exceeds the number of moles of reactants (positive change in stoichiometric mole number), entropy generally increases because of greater molecular disorder [21].

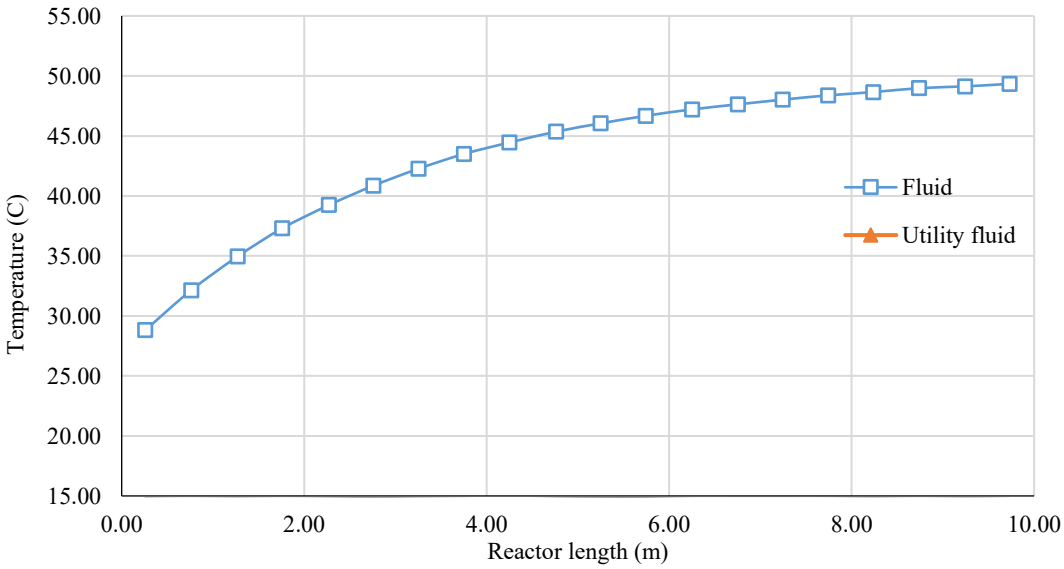

Figure 5. Temperature versus reactor length.

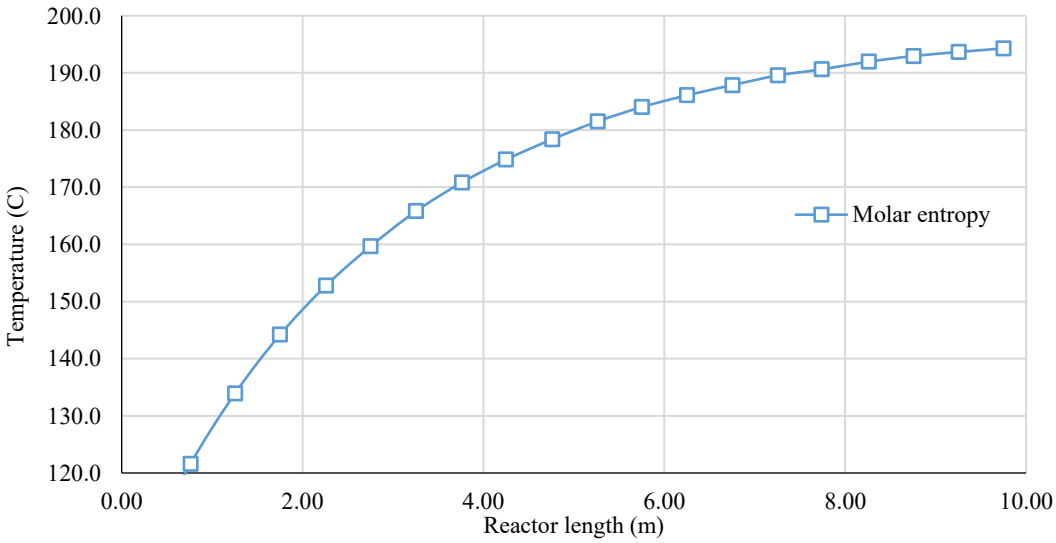

Figure 6. Molar entropy versus reactor length.

© STM Journals 2025. All Rights Reserved

In Figure 7, the volumetric flow rate of the reacting mixture does not always remain constant along the reactor length; instead, it often changes due to variations in temperature, pressure, and the number of moles present as the reaction progresses. The profile of volumetric flow rate against reactor length provides valuable insight into the fluid dynamics and mass transport characteristics of the system. For gas-phase reactions, the volumetric flow rate is strongly influenced by the ideal gas law. As the reaction advances, two key factors drive changes in flow rate: changes in total moles and changes in temperature. In an exothermic reaction, the temperature of the system increases, thereby increasing the volume occupied by the gas mixture at constant pressure. For instance, if the inlet flow rate is 0.010 m^3/s at 300 K and 5 atm, and the temperature rises to 350 K at the outlet while pressure drops slightly to 4.5 atm, the outlet volumetric flow rate can increase to nearly 0.0128 m^3/s. This expansion directly affects the residence time of the gas within the reactor and, consequently, the conversion [22].

In Figure 8, the viscosity of the reacting mixture often changes along the reactor length due to variations in temperature, composition, and phase behavior as the reaction progresses. The viscosity profile provides important insight into the fluid mechanics of the system because viscosity directly influences flow resistance, pressure drop, and mixing efficiency. A common trend observed in many gas-phase or liquid-phase PFRs is that viscosity decreases with reactor length, particularly when the reaction is accompanied by heating or the formation of lower-viscosity products. For gas-phase reactions, viscosity is a function of temperature and molecular weight distribution. As the reaction proceeds and the temperature increases, the viscosity of gases tends to rise slightly with temperature, but the effect is generally weak compared to liquids. More significant is the change in the composition of the mixture. If the products formed have lower molecular weights than the reactants, the overall gas mixture becomes less viscous. For example, in the thermal cracking of heavy hydrocarbons, the reactant may have a viscosity near 0.8 cP at 500 K, but as smaller gaseous products such as methane and ethylene are formed, the viscosity may fall to about 0.4–0.5 cP by the outlet. Thus, the viscosity profile decreases steadily along the reactor length. For liquid-phase reactions, viscosity changes are often much more pronounced. Liquids generally exhibit a strong temperature dependence of viscosity, with higher temperatures significantly reducing resistance to flow. In an exothermic reaction where the temperature rises from 300 to 350 K along the reactor, a liquid reactant mixture with an initial viscosity of 2.0 cP might decrease to about 1.2 cP. In addition, compositional changes further alter viscosity. For instance, in polymer degradation or esterification processes, the consumption of more viscous reactants and the formation of lighter products lead to a net decrease in viscosity. Conversely, in polymerization reactions, the opposite trend may be observed, with viscosity increasing as large molecules form, but in the present case, the graph shows a decreasing profile, implying the system is breaking down heavier species or being heated. The decreasing viscosity profile has several important design and operational implications [23].

In Figure 9, the density of the reacting mixture often decreases with reactor length, particularly in gas-phase reactions where temperature rises and molecular composition changes occur. Density is defined as mass per unit volume, and in flowing systems, it is directly related to the ideal gas law, where P is pressure, M is molar mass, R is the gas constant, and T is temperature. As the reaction progresses along the reactor length, both temperature and molar composition evolve, resulting in a continuous change in density. For exothermic gas-phase reactions, the most common trend is a decrease in density due to the combined effect of rising temperature and, in many cases, increasing volumetric flow from positive mole change.

For endothermic reactions, the density change depends on whether external heating is supplied. If the system absorbs heat and cools, the density may increase locally due to temperature reduction, but if the stoichiometry generates more gaseous moles, the overall density still tends to decrease. For liquid-phase systems, the density changes are generally smaller but still significant in cases where temperature rises due to exothermic reactions. Liquids typically exhibit thermal expansion coefficients that lead to a density reduction with increasing temperature. For instance, an organic reactant with an inlet density of 950 kg/m^3 at 300 K may decrease to about 930 kg/m^3 at 350 K. If lighter liquid products or gaseous byproducts are generated, this effect is amplified, leading to a clear decreasing profile along the reactor length [24].

© STM Journals 2025. All Rights Reserved

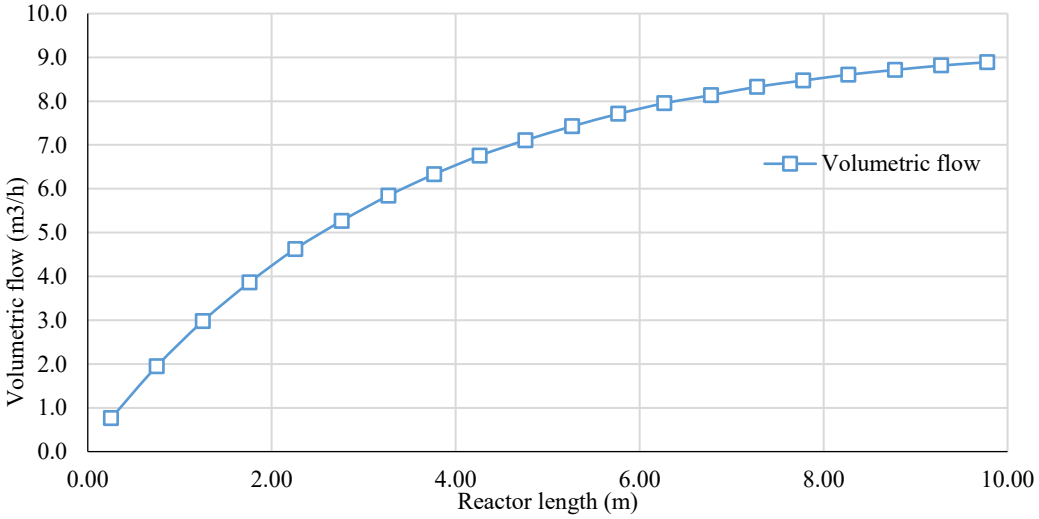

Figure 7. Volumetric flow rate versus reactor length.

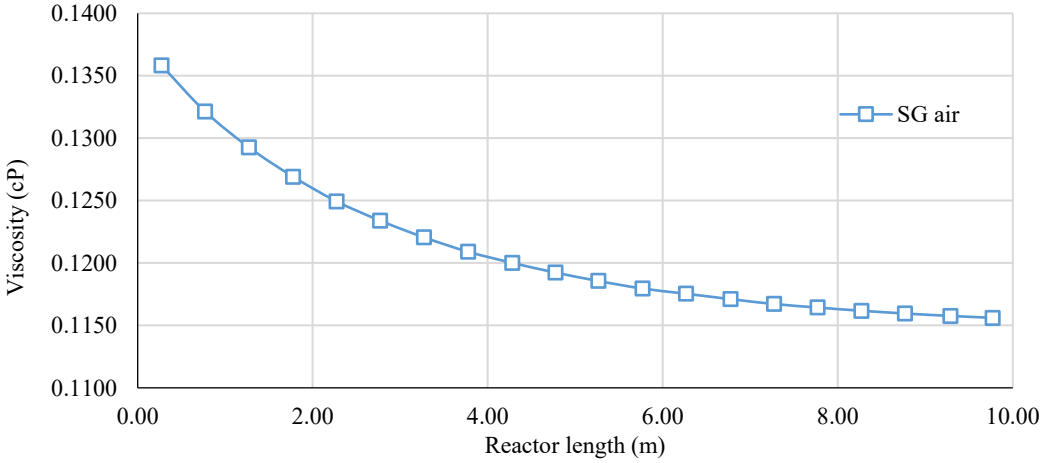

Figure 8. Viscosity versus reactor length.

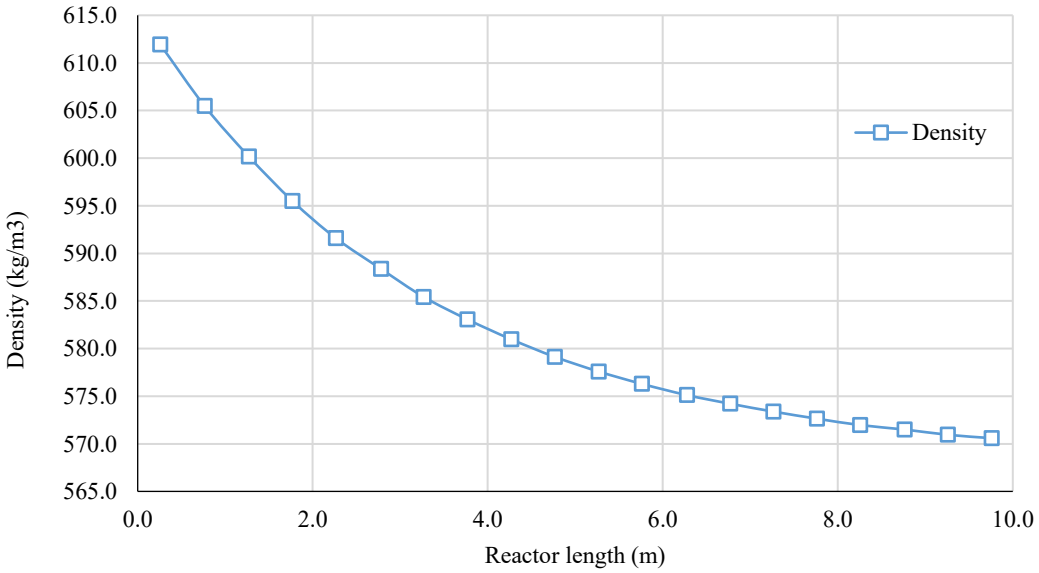

Figure 9. Density versus reactor length.

© STM Journals 2025. All Rights Reserved

In Figure 10, the molar or specific heat capacity of the reacting mixture often varies along the reactor length due to changes in temperature and composition. Heat capacity, Cp represents the amount of heat required to raise the temperature of one mole (or unit mass) of a substance by one degree Kelvin at constant pressure. The profile of heat capacity versus reactor length provides insight into how the thermal properties of the reacting mixture evolve as the reaction progresses. In many cases, the graph shows an increasing trend, reflecting either rising temperature, the formation of new products with higher heat capacities, or both. For gas-phase systems, heat capacity is strongly dependent on both temperature and molecular composition. The Shomate or polynomial form of Cp indicates that Cp increases approximately linearly with temperature for most gases over moderate temperature ranges. For example, a mixture entering the reactor at 300 K with an average molar heat capacity of 30 J/mol.K may experience a temperature rise to 350 K, resulting in an outlet heat capacity of about 35–37 J/mol.K. This increase is attributable to the fact that, at higher temperatures, additional vibrational degrees of freedom are excited, allowing the gas molecules to absorb more energy. Furthermore, if the reaction generates lighter gases such as hydrogen, carbon dioxide, or steam, species with relatively high heat capacities, the overall mixture Cp increases further. For liquid-phase reactions, the trend is similar, though the temperature dependence of heat capacity is usually weaker compared to gases. However, compositional changes can still lead to noticeable increases. In an esterification reaction, for example, the products may have higher specific heat capacities than the reactants, causing the overall mixture to exhibit an upward trend along the reactor length. A liquid mixture starting with an average Cp of 2.5 kJ/kg.K may increase to 3.0 kJ/kg.K after significant reaction progress and a modest rise in temperature. The increase in heat capacity has direct implications for thermal management in reactors. A higher heat capacity means the system can absorb more heat for a given temperature rise, which tends to moderate temperature fluctuations [25].

In Figure 11, the surface tension of the reacting mixture often decreases along the reactor length as the reaction progresses. Surface tension, defined as the energy required to increase the surface area of a liquid by a unit amount, reflects the strength of intermolecular forces within the fluid. In multiphase or liquid-phase reactions, this property is particularly important because it governs bubble formation, droplet behavior, and interfacial mass transfer. The observed decreasing profile of surface tension with reactor length typically arises from both thermal effects and compositional changes within the mixture. Temperature plays a central role in reducing surface tension. For most liquids, surface tension decreases

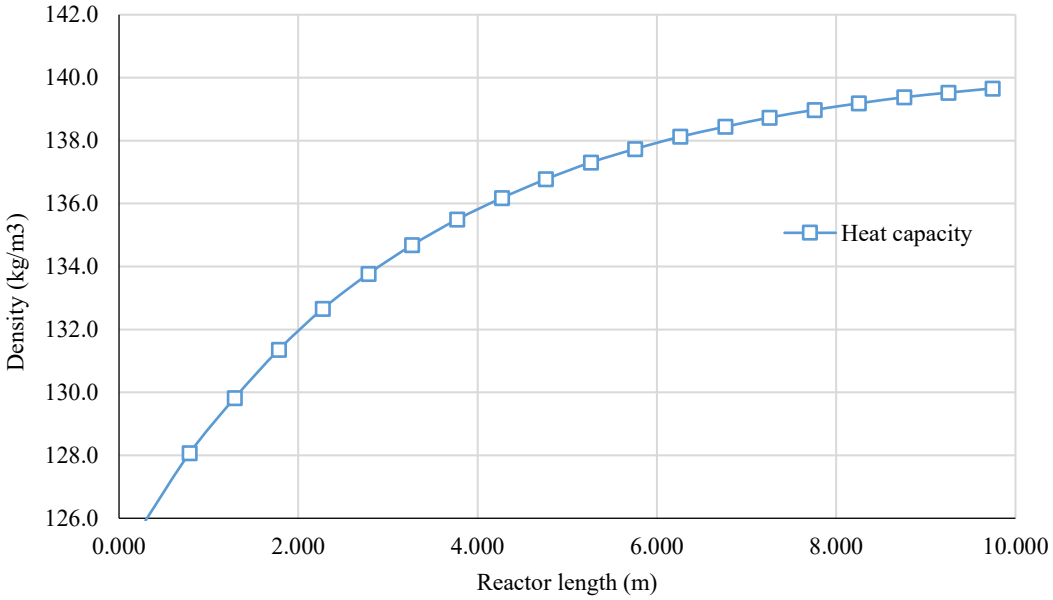

Figure 10. Heat capacity versus reactor length.

© STM Journals 2025. All Rights Reserved

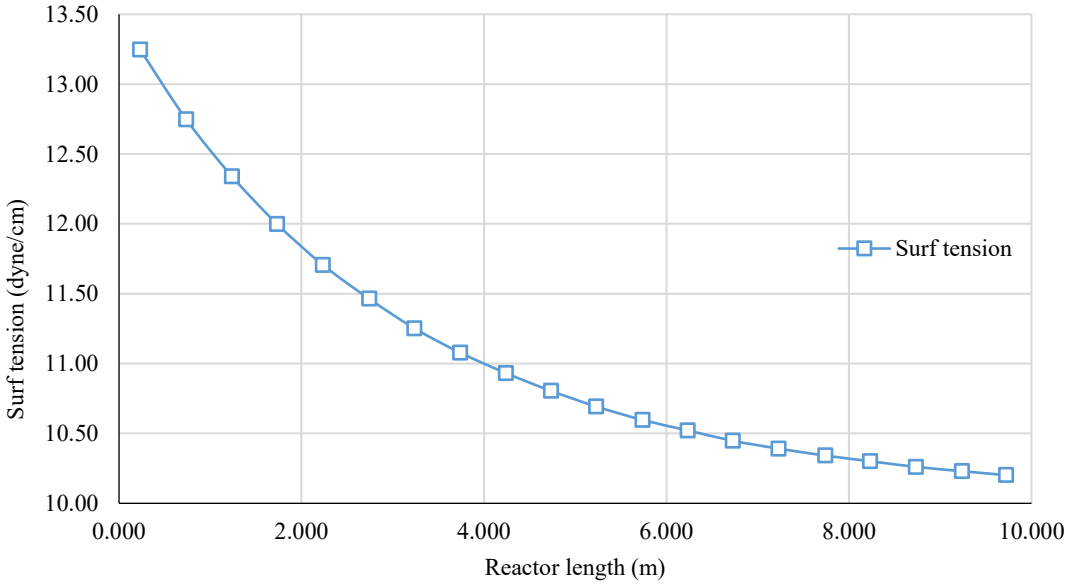

Figure 11. Surface tension versus reactor length.

In Figure 11, the surface tension of the reacting mixture often decreases along the reactor length as the reaction progresses. Surface tension, defined as the energy required to increase the surface area of a liquid by a unit amount, reflects the strength of intermolecular forces within the fluid. In multiphase or liquid-phase reactions, this property is particularly important because it governs bubble formation, droplet behavior, and interfacial mass transfer. The observed decreasing profile of surface tension with reactor length typically arises from both thermal effects and compositional changes within the mixture. Temperature plays a central role in reducing surface tension. For most liquids, surface tension decreases approximately linearly with increasing temperature, approaching zero near the critical point. For example, water has a surface tension of about 72 mN/m at 25°C (298 K), but this value decreases to around 59 mN/m at 100°C (373 K). In a PFR where an exothermic reaction raises the temperature by 50 K along the reactor, the surface tension of the mixture may fall by 10–15% depending on the fluid properties. This trend is reflected in the profile, showing a steady decline as heat release increases the average molecular energy and weakens cohesive forces at the liquid interface [26].

CONCLUSION

The first part of this work considered the development of existing kinetics of DMC production, direct synthesis of CO_2 and methanol from the literature. The reactions involved three steps: the first reaction was the reaction of methane and CO_2 to produce CO and hydrogen, the second reaction was the reaction of CO and hydrogen to produce methanol, and the final reaction was the reaction of methanol and CO_2 to produce DMC and water. After the development of the kinetics, the mathematical model of a packed bed reactor was then developed from the principles of conservation of mass and energy.

The second part of this work considered the simulation of the DMC plant to produce 30,000 t per year using Aspen HYSYS software. The simulation started by compressing natural gas, which was cooled and sent to a separator to separate out methane from the other gases. The methane from the separator was then mixed with a stream of CO_2 gas and sent to the first reactor, where the reaction of methane and CO_2 to produce CO and hydrogen occurred. The product from the first reactor was then heated before being sent to the second reactor, where the reaction of CO and hydrogen to produce methanol occurred. The outlet from the second reactor was sent to a second separator, where pure methanol was separated and mixed with a second stream of CO_2 before entering the DMC reactor, where the production of DMC took place. The outlet of the DMC reactor was sent to the final separator, where pure DMC was recovered and sent to a storage tank.

© STM Journals 2025. All Rights Reserved

The third part of this work considered the material and energy balance of each unit of the DMC plant, such as: compressor, heater, separator, mixer, PFR1, cooler, PFR2, separator 2, mixer 2, DMC reactor, separator 3, and tank. The fourth part of this work considered the sizing of various equipment of the DMC plant, such as: compressor, heater, separator, mixer, PFR1, cooler, PFR2, separator2, mixer 2, DMC reactor, separator 3, and tank. The fifth part of this work considered the process optimization of the DMC product by determining the optimum conversion of methanol that gives the optimum yield of DMC product. The DMC was produced at the conversion reactor, where methanol and CO_2 were synthesized at a temperature and pressure of 162.7°C and 60 bar, respectively. The optimization and gas revealed that an 80% methanol conversion rate yielded the highest DMC production, beyond which the yield decreased to equilibrium constraints. Finally, the last part of this work considered the economic analysis of the DMC plant in terms of costing the major equipment in the plant. For the cost estimation and economic evaluation for the first year, an estimated capital investment of approximately 2,823,220 USD and operating costs of 1,506,050 USD/year will be required. The establishment of the plant is anticipated to yield encompassing job creation, increased tax revenue, and local economic development. Overall, the proposed project plant holds significant potential and annually produces 30,000 t of 95% pure DMC from natural gas.

REFERENCES

1. Adegoriola AE, Suleiman IM. Adopting Gas Automobile Fuels (LPG and CNG) into the Nigerian Transportation System. J Econ Sustain Dev. 2020; 10(14): 12–19.
2. Arteconi A, Mazzarini A, Nicola GD. Emissions from ethers and organic Carbonate Fuel Additives: A Review. Water Air Soil Pollut. 2011; 221(1–4): 405–423.
3. Babi DK. Teaching Sustainable Process Design using 12 systematic Computer-Aided Tasks. Comput-Aided Chem Eng. 2015; 37: 173–178.
4. Baggio L, Govaert M, Marchal B, Rouxhet A. Direct Dimethyl Carbonate Production from Carbon Dioxide and Methanol. University of Liege Eurecha; 2022; 2–17.
5. Chibuzo EB. Gas flaring and rainwater composition – a negative synergy: a case study of Utorogu Community in Niger Delta, Nigeria. J Environ Soc Sci. 2016;3(2):124–132.
6. Bruno TJ, Wolk A, Naydich A, Huber ML. Composition-explicit distillation curves for mixtures of diesel fuel with dimethyl carbonate and diethyl carbonate. Energy Fuels. 2009;23(8):3989–97. doi:10.1021/ef900215v.
7. Challa P, Paleti G, Madduluri VR, Gadamani SB, Pothu R, Burri DR, Boddula R, Perugopu V, Kamaraju SRR. Trends in emission and utilization of CO_2: Sustainable feedstock in the synthesis of value-added fine chemicals. Catal Surv Asia. 2022;26(2):80–91. doi:10.1007/s10563-021-09352-6.
8. Cheung CS, Zhu RJ, Huang ZH. Investigation on the gaseous and particulate emissions of a compression ignition engine fueled with diesel-dimethyl carbonate blends. Sci Total Environ. 2011; 409(3): 523–529.
9. De Groot FFT, Lammerink RRGJ, Heidemann C, van der Werff MPM, Garcia TC, van der Ham LAGJ, van den Berg H. The industrial production of dimethyl carbonate from methanol and carbon dioxide. Chem Eng Trans. 2014; 39: 1561–1566. DOI:10.3303/CET14392611562.
10. Dong-Hwi J, Yun-Gyu L, Hyeong Uk L, Jae ML, Na-Young K. Design of Dimethyl Carbonate (DMC) synthesis process using CO_2, techno-economic analysis and life cycle assessment. Research Square. 2023; 1–27. DOI: https://doi.org/10.21203/rs.3.rs-3390777/v1.
11. Gong YF, Liu SH, Guo HJ, Hu TG, Zhou LB. A new diesel oxygenates additive and its effects on engine combustion and emissions. Appl Therm Eng. 2021; 27(1): 202–207.
12. Hou Z, Han B, Liu Z, Jiang T, Yang G. Synthesis of dimethyl carbonate using CO_2 and methanol: Enhancing the conversion by controlling the phase behavior. Green Chem. 2022; 4(5): 467–471.
13. Huang H, Samsun RC, Peters R, Stolten D. Greener production of dimethyl carbonate by the Power-to-Fuel concept: a comparative technoeconomic analysis. Green Chem. 2021; 23(4): 1734–1747.
14. International Energy Agency. The Future of Trucks: Implications for Energy and the Environment, Paris: IEA; 2023. doi:10.1787/9789264279452-en.

© STM Journals 2025. All Rights Reserved

15. IPCC. Climate Change (2022): Impacts; Adaptation and Vulnerability. Working Group II contribution to the IPCC Sixth Assessment Report. 2022.
16. Kitagawa H, Murayama T, Tosaka S, Fujiwara Y. The effect of oxygenated fuel additive on the reduction of diesel exhaust particulates. SAE paper 2001-01-2020. 2001.
17. Kohli K, Sharma BK, Panchal CB. Dimethyl Carbonate: Review of Synthesis Routes and Catalysts Used. Energies. 2022; 15(14): 5133. https://doi.org/10.3390/en15145133.
18. Kongpanna P, Pavarajarn V, Gani R, Assabumrungrat S. Techno-economic evaluation of different CO_2-based processes for dimethyl carbonate production. Chem Eng Res Des. 2015; 93: 496–510.
19. Kreutzberger CB. Chloroformates and Carbonates. In: Kirk-Othmer Encyclopedia of Chemical Technology. Wiley; 2001.
20. Mei D, Hielscher K, Baar R. Study on combustion process and emissions of a single-cylinder diesel engine fueled with DMC/diesel blend. J Energy Eng. 2014; 140(1): 04013004.
21. Morgan T. Autogas Incentive Policies: A Country-By-Country Analysis of Why and How Governments Encourage Autogas and What Works. Brussels, Belgium: European LPG Association. 2024.
22. Naujoks J, Sakthi Nallasivam SM, Venkatesh N, Jhamb S. (189n) A Systematic Process Design for Sustainable Dimethyl Carbonate Production through Carbon Dioxide Utilization. 2017 AIChE Annual Meeting, Minneapolis, Minnesota, United States. 2017.
23. Navas-Anguita Z, García-Gusano D, Iribarren D. A review of techno-economic data for road transportation fuels. Renew Sustain Energy Rev. 2019; 112: 11–26.
24. Pacheco MA, Marshall CL. Review of dimethyl carbonate (DMC) manufacture and its characteristics as a fuel additive. Energy Fuels. 2020; 11(1): 2–29.
25. Perugopu RV, Kamaraju SRR. Trends in emission and utilization of CO_2: Sustainable feedstock in the synthesis of value-added fine chemicals. Catal Surv Asia. 2022; 26(2): 80–91.
26. Pilavachi PA, Schenk M, Perez-Cisneros E, Gani R. Modeling and simulation of reactive distillation operations. Ind Eng Chem Res. 1997;36(8):3188–94. doi:10.1021/ie9606404.

© STM Journals 2025. All Rights Reserved